

Shahram Roshanpour

DEVELOPMENT A MATHEMATICAL MODEL OF PROCESSES INSIDE RF HOLLOW CATHODE TAKING VISCOSITY INTO ACCOUNT IN ELECTRON DYNAMICS

The object of research is high-frequency hollow cathode as electron sources in plasma-ion thrusters and Hall effect thrusters with relatively low-power.

Publications devoted to high-frequency (helicon) thrusters consider Trivelpiece-Gould waves, helicon waves, as well as ion-cyclotron and electron-cyclotron resonance, as mechanisms for absorbing electromagnetic energy. In this case, electron scattering by atoms and ions within the thruster channel is considered a factor in plasma thermalization. The discharge conditions and the dimensions of the low-power cathode cavity virtually eliminate the occurrence of these effects, while significantly enhancing the relaxation of electron momentum due to non-mirror reflection from the potential barrier in the boundary bipolar layer. The parameters describing the results of this reflection within the cavity volume are the axial-azimuth and radial-azimuth components of the electron viscosity tensor, corresponding to the electron momentum flux in the direction of zero mass flow. It is shown that viscous electron momentum transport facilitates magnetic field penetration deeper into the plasma than is predicted by classical skin-layer theory, which considers the relaxation of electrons motion only because of collisions in the volume. Conditions under which rotation-cyclotron resonance is possible are identified. The input of viscosity into electrons thermalization process is shown.

The results obtained in the work can be used in predicting operating parameters and narrowing the range of parameter variations when developing laboratory models.

Keywords: high-frequency cathode, viscosity tensor, potential barrier, skin-layer, bipolar layer.

Received: 11.01.2026

Received in revised form: 21.03.2026

Accepted: 01.04.2026

Published: 30.04.2026

© The Author(s) 2026

This is an open access article

under the Creative Commons CC BY license

<https://creativecommons.org/licenses/by/4.0/>

How to cite

Roshanpour, S. (2026). Development a mathematical model of processes inside RF hollow cathode taking viscosity into account in electron dynamics. *Technology Audit and Production Reserves*, 2 (1 (88)), 64–69. <https://doi.org/10.15587/2706-5448.2026.356937>

1. Introduction

The expansion of astronautics tasks at last decade of XX century has resulted in creation of the whole series of narrowly specialized satellites, as on an example CubeSat, with small mass and simultaneously low power produced by solar arrays. The samples of electric propulsion thrusters, developed before used for orbits correction and operating in a mode of the arc discharge, were characterized by increase of thrust power cost at reduction of scale parameters of the thruster.

Ablative pulse plasma thrusters [1] and plasma-ion thrusters (PIT) with high-frequency (HF) ionization [2] proved to be satisfactory in terms of life-time at low thrusts and powers. Also, the use of RF cathodes as electron sources for PIT ionization chambers and neutralizers in PIT and Hall effect thrusters (HET) made it possible to reduce the electron power cost at low thrust levels.

1. The paper [3] represents ion cyclotron resonance (ICR) in which the cyclotron frequency of ions in the constant component of the magnetic field coincides with the frequency of the time-varying component of the magnetic field. However, the realization of such a resonance is possible only by chance in limited volumes, since, unlike the time-variable component, the cyclotron frequency in the constant component depends on the coordinate.

2. The paper [4] represents electron cyclotron (ECR) resonance – a similar coincidence exists in ion dynamics and with the same property of randomness and limited space.

3. The paper [5] represents helicon (spiral) low-frequency electromagnetic waves that arise and propagate with relatively weak attenuation in metallic conductors and plasma placed in an external magnetic field. In this case, however, as in all works related to helicon thrusters, the propagation of helicon waves is described by expressions that are valid only in unlimited space with a uniform distribution of plasma parameters.

4. The paper [6] represents low-frequency potential Trivelpiece-Gould waves excited by helicon waves, which strongly damp and heat the plasma. Just as in work [5], quantitative characteristics were found for a homogeneous plasma in an unlimited space.

The paper [7] represents skin effect, also responsible for the functioning of high-frequency devices, but, as in all known classical expressions, it describes the skin effect without taking into account the viscous transfer of momentum along and across the magnetic lines.

The description of the processes in the listed works does not relate to the specifics of hollow RF cathodes, is of a general theoretical nature and is not implemented in mathematical models and calculation methods.

The work [8] presents the results of the development of high-frequency hollow cathodes for processing large-area double-sided foil in

a pressure range ten of times greater than those typical for cathodes of electric propulsion thrusters.

The work [9] presents the results of the development of a high-frequency hollow cathode for use in a plasma-chemical reactor at electron current values significantly higher than in hollow cathodes of electric propulsion thrusters.

The work [10] is devoted to the development of a hollow RF cathode-neutralizer for a plasma-ion thruster, containing only the results of an experimental research.

A common characteristic of these studies is that they consider particle scattering only within the volume, the effect of which is negligible in the case of cathode sizes small compared to thrusters. At small sizes, the relaxation of electron momentum as a result of their non-mirror reflection from the potential barrier in the bipolar layer adjacent to the plasma becomes significant [11].

All this allows to state that it is advisable to conduct a research devoted to development of mathematic model of viscous electron momentum transport in electric propulsion devices with closed electron drift. The relevance of this research stems from the lack of consideration in existing mathematical models of the specific of electrons momentum transport in rarefied plasma under action of magnetic field and at presence of potential barrier inside boundary bipolar layer.

The aim of research is to develop a mathematical model of processes inside radio-frequency (RF) hollow cathode taking viscosity into account in electron dynamics. The objectives of research are:

1. To write the azimuth projection of the electron motion equation, taking into account the influence of a magnetic field on viscous momentum transport and viscous components of the electrons momentum flux density.
2. To write the equation of radial-azimuth component of electrons viscosity tensor.
3. To write the expressions for electrons energy equation compounds, which represent the input of viscosity into process of electrons thermalization.

2. Materials and Methods

2.1. Current state

The object of research is high-frequency hollow cathode as electron sources in plasma-ion thrusters and Hall effect thrusters with relatively low-power.

The following scientific methods were used in the research:

- analysis method when studying existing models of processes in high-frequency electric propulsion devices, with the determination of the limits of their applicability in the rarefied plasma of high-frequency hollow cathodes at relatively low currents;
- theoretical methods in formulating a mathematical model of viscous momentum transport and its integration into a comprehensive mathematical model of processes in a high-frequency hollow cathode of a low-power electric propulsion thruster.

The use of high-frequency discharge is also proposed directly in thrusters called "helicon" ones (Fig. 1).

Here the acceleration of the propellant is the result of the following series of processes: alternating azimuth current in the inductor $I_i \rightarrow$ alternating axially symmetric magnetic field $i_x B_x + i_r B_r \rightarrow$ alternating azimuth electric field $j_\psi E_\psi \rightarrow$ alternating azimuth current $j_\psi \rightarrow$ axial force F_x as a result of the interaction $j_\psi B_r$.

Here $I_i, B_x, B_r, E_\psi, j_\psi$ are periodic and alternating with zero average values for one period of the source. But the product $j_\psi B_r$ and, accordingly, the axial force F_x remain to be of constant sign – the processes listed above are sufficient to create the thrust. However, some mechanism for relaxing the azimuth projection of the electron momentum is necessary, since in the absence of resistance factors, the inductor's

magnetic field does not penetrate the plasma. Ionization of the propellant is also impossible, which is especially important in the case of a HF electron source.

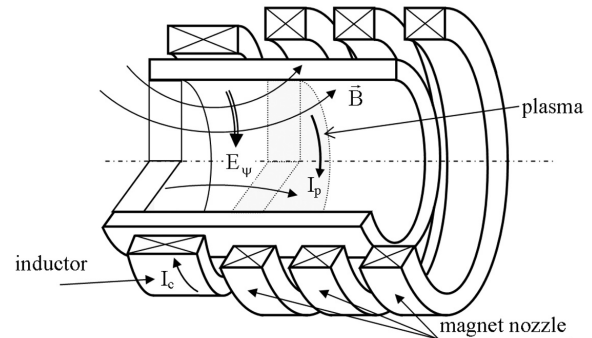


Fig. 1. Helicon thruster

When describing processes in conductors (including plasma) in a time-varying magnetic field, the concept of a skin layer [7] arises, which is determined by the following series of processes (Fig. 1):

- a time-varying external magnetic field created by a current I_c in an inductor, which induces a time-varying electric field in the conductor;
- the induced electric field excites a current I_p in the conductor opposite in direction to the current I_c ;
- the current excited by the electric field creates a magnetic field opposite in sign to the external field.

As a result, it turns out that in the direction deep into the conductor, the magnetic field weakens more intensively, the higher the conductivity – significant values of the magnetic field are present in the surface layer – the magnetic layer, the skin layer. The depth of the skin layer is usually determined from the following considerations.

The azimuth projection of the electrons motion equation in classic theory of skin layer has the form

$$m_e n_e \left(\frac{\partial V_{e\psi}}{\partial t} + \frac{V_{e\psi}}{\tau_e^{(r)}} \right) + e n_e (E_\psi - V_{e\psi} B) = 0, \quad (1)$$

where $n_e, V_{e\psi}$ – population and azimuth projection of the mass-averaged electron velocity.

Neglecting viscosity, equation (1) takes on a simplified form

$$\frac{1}{v_e^{(p)}} \frac{\partial j_\psi}{\partial t} + j_\psi \approx \sigma_p E_\psi, \quad (2)$$

where $\vec{j} = -en_e \vec{V}_e$ – electron current density; σ_p – plasma conductivity

$$\sigma_p = \frac{e^2 n_e}{m_e v_e^{(p)}}. \quad (3)$$

If the electric field strength varies in time harmonically with frequency and amplitude $E_{\psi A}$, the current density will also vary harmonically with amplitude $j_{\psi A}$, equal to

$$j_{\psi A} = \frac{\sigma_p E_{\psi A}}{\sqrt{1 + \left(\frac{\omega}{v_e^{(p)}} \right)^2}}. \quad (4)$$

Thus, the description in neglect of viscosity shows the proportion between the amplitudes of the current and the electric field strength. The maximum $E_{\psi A}$ at the periphery with attenuation deep into the channel means the same $j_{\psi A}$ behavior.

The vector potential, magnetic induction and, accordingly, the electric current when deepening into the conductor have the form of decaying waves with a decrement of attenuation and a wavelength of the δ_s order

$$\delta_s = \sqrt{\frac{\epsilon_0 c^2}{\omega \sigma_p}}. \quad (5)$$

The depth of the skin layer can often be small compared to the size of the discharge volume – ionization occurs in the peripheral region of the discharge, and the central region is filled with ions and electrons due to their diffusion from the peripheral region.

In ground-based applications, in technological plasma systems with a stagnant atmosphere, plasma generation only at the periphery of the discharge is not a problem. In electric propulsion thrusters (expenditure systems) and their components (e. g., cathodes), such a phenomenon would mean an unacceptable reduction in specific impulse and efficiency – the neutral component from the central region would exit the device channel, not participating in the generation of ions and electrons.

For hollow RF cathodes with relatively low power and small cavity dimensions, the scattering effect within the volume is negligible. Moreover, the cavity's nearly closed volume, opened by a small-diameter orifice, eliminates the presence of traveling waves, such as helicon waves and Trivelpiece-Gould waves. Significant in this case are the boundary processes of electron momentum relaxation as a result of non-mirror reflection from the potential barrier in the bipolar layer bordering the plasma [11]. In gas dynamics, this process is represented by the axial-azimuth ($\pi_{es}^{(x\psi)}$) and radial-azimuth $\pi_{es}^{(r\psi)}$ components of the viscosity tensor.

2.2. Formation of equations set

A mathematical model of viscous momentum transport in a high-frequency hollow cathode has been developed as a component of the first developed holistic plasma dynamic model based on the compromise kinetic-fluid method [12] using the boundary conditions for the transport of momentum and electron energy formulated in it in the presence of potential barriers in the bipolar layer boundary with the plasma.

The dependence of magnetic induction on time at the upper boundary of the plasma (Fig. 2) can be written as follows

$$B(R) = B_s(R) \sin \omega_l t, \quad (6)$$

where ω_l – circular frequency of the inductor.

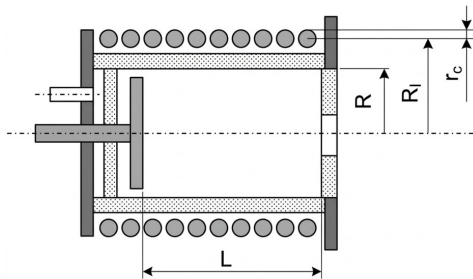


Fig. 2. Cathode cavity configuration

When moving deep into the plasma, the phase of oscillations shifts against (6):

$$B = B_s \sin \omega_l t + B_c \cos \omega_l t; \quad (7)$$

$$E_\psi = E_s \sin \omega_l t + E_c \cos \omega_l t; \quad (8)$$

$$j_\psi = j_s \sin \omega_l t + j_c \cos \omega_l t; \quad (9)$$

$$V_{c\psi} = V_{es} \sin \omega_l t + V_{ec} \cos \omega_l t. \quad (10)$$

Considering the axial projection \vec{B} and azimuth projections \vec{j} and \vec{A} as the main ones, it is possible to write:

$$\frac{1}{r} \frac{\partial}{\partial r} (E_\psi r) = -\frac{\partial B}{\partial t}, \quad (11)$$

$$\frac{\partial B}{\partial r} = \frac{\partial}{\partial r} \left(\frac{1}{r} \frac{\partial}{\partial r} (Ar) \right) = -\frac{j}{\epsilon_0 c^2}. \quad (12)$$

In this case at each point in the volume of the cavity:

$$\frac{1}{r} \frac{\partial}{\partial r} (E_s r) = -\omega_l B_c, \quad (13)$$

$$\frac{1}{r} \frac{\partial}{\partial r} (E_c r) = \omega_l B_s, \quad (14)$$

$$\frac{\partial B_s}{\partial r} = \frac{en_e V_{es}}{\epsilon_0 c^2}, \quad (15)$$

$$\frac{\partial B_c}{\partial r} = \frac{en_e V_{ec}}{\epsilon_0 c^2}. \quad (16)$$

One can notice the in-phase change in the values of magnetic induction and the azimuth projection of the electrons mass flux velocity.

3. Results and Discussions

3.1. The azimuth projection of electrons motion equation

The electrons motion equation can be written in the zero-mass approximation of the electron, preserving non-stationarity and momentum loss in collisions only for the azimuth projection

$$m_e n_e \left(\frac{\partial V_{e\psi}}{\partial t} + \frac{V_{e\psi}}{\tau_e^{(tr)}} \right) + \frac{\partial \pi_e^{(x\psi)}}{\partial x} + \frac{1}{r^2} \frac{\partial}{\partial r} (\pi_e^{(r\psi)} r^2) + en_e (E_\psi - V_{er} B) = 0. \quad (17)$$

Closing the system of equations requires approximate notations for the dissipative quantity π . Using expression results of [11], it is possible to write

$$\frac{\partial \pi_e^{(x\psi)}}{\partial x} \approx \frac{\pi_{e+}^{(x\psi)} - \pi_{e-}^{(x\psi)}}{L} \approx \frac{m_e n_e \eta_e^{(p)} v_e V_{e\psi}}{2L}, \quad (18)$$

where L – the length of the cathode cavity; $\eta_e^{(p)}$ – effective coefficient of electrons momentum relaxation because of non-mirror reflection of potential barrier.

In this case, for the azimuth projection of the equation of motion (17) and for the pressure scalar equation

$$m_e n_e \left(\frac{\partial V_{e\psi}}{\partial t} + \frac{V_{e\psi}}{\tau_{e\Sigma}^{(tr)}} \right) + \frac{1}{r^2} \frac{\partial}{\partial r} (\pi_e^{(r\psi)} r^2) + en_e (E_\psi - V_{er} B) = 0, \quad (19)$$

where $\tau_{e\Sigma}^{(tr)}$ – effective time of electrons momentum relaxation

$$\frac{1}{\tau_{e\Sigma}^{(tr)}} = \frac{1}{\tau_e^{(tr)}} + \frac{\eta_e^{(p)} v_e}{2L}. \quad (20)$$

Substituting (8)–(14) into (19) allows to write:

$$m_e n_e \left(-\omega_l V_{ec} + \frac{V_{es}}{\tau_{e\Sigma}^{(tr)}} \right) + \frac{1}{r^2} \frac{\partial}{\partial r} (\pi_{es}^{(r\psi)} r^2) + en_e (E_s - V_{er} B_s) = 0, \quad (21)$$

$$m_e n_e \left(\omega_l V_{es} + \frac{V_{ec}}{\tau_{e\Sigma}^{(tr)}} \right) + \frac{1}{r^2} \frac{\partial}{\partial r} \left(\pi_{ec}^{(r\psi)} r^2 \right) + e n_e (E_c - V_{er} B_c) = 0, \quad (22)$$

and

$$m_e n_e V_{es} = - \frac{\tau_{e\Sigma}^{(tr)}}{1 + (\omega_l \tau_{e\Sigma}^{(tr)})^2} \left(\left(\frac{1}{r^2} \frac{\partial}{\partial r} \left(\pi_{es}^{(r\psi)} r^2 \right) + e n_e (E_s - V_{er} B_s) \right) \right) + \omega_l \tau_{e\Sigma}^{(tr)} \left(\frac{1}{r^2} \frac{\partial}{\partial r} \left(\pi_{ec}^{(r\psi)} r^2 \right) + e n_e (E_c - V_{er} B_c) \right), \quad (23)$$

$$m_e n_e V_{ec} = - \frac{\tau_{e\Sigma}^{(tr)}}{1 + (\omega_l \tau_{e\Sigma}^{(tr)})^2} \left(\left(\frac{1}{r^2} \frac{\partial}{\partial r} \left(\pi_{ec}^{(r\psi)} r^2 \right) + e n_e (E_c - V_{er} B_c) \right) - \omega_l \tau_{e\Sigma}^{(tr)} \left(\frac{1}{r^2} \frac{\partial}{\partial r} \left(\pi_{es}^{(r\psi)} r^2 \right) + e n_e (E_s - V_{er} B_s) \right) \right), \quad (24)$$

when

$$\pi_e^{(r\psi)} = \pi_{es}^{(r\psi)} \sin \omega_l t + \pi_{ec}^{(r\psi)} \cos \omega_l t. \quad (25)$$

In writing the equation of the radial-azimuth component $\pi_e^{(r\psi)}$ of the viscosity tensor for an arbitrary point in the volume of the cavity, it is convenient to represent expressions (7), (10) as follows:

$$V_{e\psi} = V_{es} \sin \omega_l t + V_{ec} \cos \omega_l t = V_{ea} \sin \vartheta, \quad (26)$$

$$B = B_s \sin \omega_l t + B_c \cos \omega_l t = B_a \sin \vartheta, \quad (27)$$

where

$$V_{ea} = \sqrt{V_{es}^2 + V_{ec}^2}, \quad B_a = \sqrt{B_s^2 + B_c^2}, \quad (28)$$

$$\vartheta = \omega_l t + \arcsin \frac{B_c}{\sqrt{B_s^2 + B_c^2}} = \omega_l t + \arcsin \frac{V_{ec}}{\sqrt{V_{es}^2 + V_{ec}^2}}. \quad (29)$$

3.2. Equation of radial-azimuth component of electrons viscosity tensor

In this case, taking into account the pressure tensor equation in work [13] and the coincidence of the off-diagonal components of the pressure and viscosity tensors

$$\begin{aligned} \omega_l \frac{\partial \pi_e^{(r\psi)}}{\partial \vartheta} + \frac{3}{2\tau_{e\Sigma}^{(d)}} \pi_e^{(r\psi)} + \omega_{l(eff)} \pi_e^{(A)} \sin \vartheta = \\ = -P_e r \frac{\partial}{\partial r} \left(\frac{V_{ea}}{r} \right) \sin \vartheta, \end{aligned} \quad (30)$$

where

$$\omega_{l(eff)} = \frac{e B_a}{m_e} - \frac{V_{ea}}{r}, \quad (31)$$

$$\pi_e^{(A)} = \pi_e^{(\psi\psi)} - \pi_e^{(rr)}. \quad (32)$$

For the complex $\pi_e^{(A)}$, taking into account [13], it is possible to write

$$\omega_l \frac{\partial \pi_e^{(A)}}{\partial \vartheta} + \frac{3}{2\tau_{e\Sigma}^{(d)}} \pi_e^{(A)} - 4\omega_{l(eff)} \pi_e^{(r\psi)} \sin \vartheta = 0. \quad (33)$$

It is possible to obtain a solution to the system of equations (30), (33) in three extreme cases:

$$\omega_{l(eff)} \rightarrow 0:$$

$$\pi_e^{(r\psi)} = - \frac{2\tau_{e\Sigma}^{(d)}}{3} P_e r \frac{\partial}{\partial r} \left(\frac{V_{ea}}{r} \right) \frac{\sin \vartheta - \chi_l \cos \vartheta}{1 + \chi_l^2}; \quad (34)$$

$$\omega_l \tau_{e\Sigma}^{(d)} \ll 1:$$

$$\pi_e^{(r\psi)} = - \frac{2\tau_{e\Sigma}^{(d)}}{3} P_e r \frac{\partial}{\partial r} \left(\frac{V_{ea}}{r} \right) \frac{\sin \vartheta}{1 + \chi_c^2 \sin^2 \vartheta}; \quad (35)$$

$$\omega_l \tau_{e\Sigma}^{(d)} \gg 1:$$

$$\pi_e^{(r\psi)} = \pi_c \cos \left(\frac{\chi_c}{\chi_l} \cos \vartheta \right) + \pi_s \sin \left(\frac{\chi_c}{\chi_l} \cos \vartheta \right), \quad (36)$$

where

$$\chi_l = \frac{2\omega_l \tau_{e\Sigma}^{(d)}}{3}, \quad \chi_c = \frac{4\omega_{l(eff)} \tau_{e\Sigma}^{(d)}}{3}. \quad (37)$$

It can be seen that in the case $\omega_l \tau_{e\Sigma}^{(d)} \gg 1$ the quantity $\pi_e^{(r\psi)}$ does not depend on any external factors, i.e. the trivial solution is $\pi_e^{(r\psi)} = 0$.

For an arbitrary case, expressions (34)–(36) can be approximately combined into one

$$\pi_e^{(r\psi)} = - \frac{2\tau_{e\Sigma}^{(d)}}{3} P_e r \frac{\partial}{\partial r} \left(\frac{V_{ea}}{r} \right) \frac{\sin \vartheta - \chi_l \cos \vartheta}{1 + \chi_l^2 + \chi_c^2 \sin^2 \vartheta}. \quad (38)$$

In this case, the average over the half-period with fixed signs $V_{e\psi}$ and B values $\pi_e^{(r\psi)}$ is equal to:

$$\frac{1}{\pi} \int_0^\pi \pi_e^{(r\psi)} d\vartheta = \frac{2}{\pi} \pi_{ea}^{(r\psi)}, \quad (39)$$

$$\pi_{ea}^{(r\psi)} = - \frac{2\tau_{e\Sigma}^{(d)}}{3} \xi_\pi^{(V)}(\chi_l, \chi_c) P_e r \frac{\partial}{\partial r} \left(\frac{V_{ea}}{r} \right), \quad (40)$$

$$\xi_\pi^{(V)}(\chi_l, \chi_c) = \frac{\ln \sqrt{1 + \chi_l^2 + \chi_c^2} + \chi_c}{\chi_c \sqrt{1 + \chi_l^2 + \chi_c^2}}, \quad (41)$$

which, when substituting equations (23)–(25), allows to write:

$$\pi_{es}^{(r\psi)} = \frac{B_s}{\sqrt{B_s^2 + B_c^2}} \pi_{ea}^{(r\psi)}, \quad (42)$$

$$\pi_{ec}^{(r\psi)} = \frac{B_c}{\sqrt{B_s^2 + B_c^2}} \pi_{ea}^{(r\psi)}. \quad (43)$$

3.3. Electrons energy equation compounds, which represent the input of viscosity into process of electrons thermalization

The average values over the period of the last two terms of the right-hand side of the electron energy equation are then defined as

$$\begin{aligned} \left\langle \frac{m_e n_e V_{e\psi}^2}{\tau_{e\Sigma}^{(tr)}} + \frac{V_{e\psi}}{r^2} \frac{\partial}{\partial r} \left(\pi_e^{(r\psi)} r^2 \right) \right\rangle = \\ = \frac{m_e n_e V_{ea}^2}{2\tau_{e\Sigma}^{(tr)}} + \frac{V_{ea}}{r^2} \frac{\partial}{\partial r} \left(\frac{\xi_\pi^{(P)}(\chi_l, \chi_c)}{\xi_\pi^{(V)}(\chi_l, \chi_c)} \pi_{ea}^{(r\psi)} r^2 \right), \end{aligned} \quad (44)$$

where

$$\xi_{\pi}^{(p)}(\chi_l, \chi_c) = \frac{1}{\pi} \int_0^{\pi} \frac{\sin^2 \vartheta d\vartheta}{1 + \chi_l^2 + \chi_c^2 \sin^2 \vartheta}. \quad (45)$$

With an error of no more than 1.5%, dependence (45) is approximated by the expression

$$\xi_{\pi}^{(p)}(\chi_l, \chi_c) = \frac{8(1 + \chi_l^2) + \chi_c^2}{16(1 + \chi_l^2)^2 + 14\chi_c^2(1 + \chi_l^2) + \chi_c^4}. \quad (46)$$

Expressions (34), (35) and (38) demonstrate a tendency to transform the electron rotation into a "solid-state" one – $V_{e\psi} \sim r$, reducing the azimuth current at the periphery and increasing – in the middle part of the cavity. The depth of penetration of the magnetic field into the plasma increases in this case [14].

Expression (31) shows in the case of $eB_a/m_e - V_{ea}/r \rightarrow 0$ a possibility of rotational-cyclotron resonance in the cylindrical layers in the cathode cavity.

Substituting expressions (44)–(46) into the electrons motion and energy equations allows to close the equation system of the mathematical model of processes in a high-frequency electron source. A promising future research opportunity is to analyze the parameters under which rotational-cyclotron resonance is possible.

The first-developed model of viscous momentum transfer in a high-frequency hollow cathode presented in this paper is incorporated into a newly developed comprehensive mathematical model and used in calculations. The calculation results are presented in [15]. In particular, a comparison is provided between the calculated current-voltage characteristic and the one measured one during testing of the high-frequency hollow cathode developed by the author (Fig. 3).

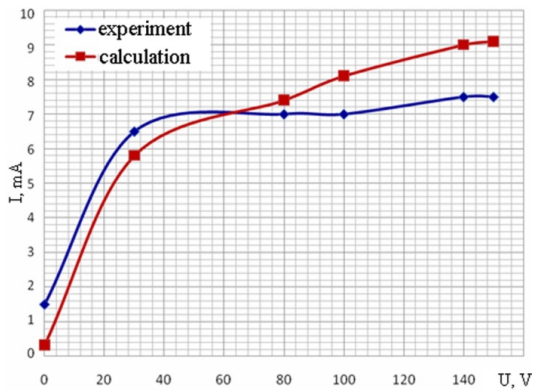


Fig. 3. Current-voltage characteristic of the cathode at a mass flow rate of 0.2 mg/s, RF power of 50 W, current in the external coil of 2.2 A

The experimental curve saturates at $I \approx 7$ mA at a voltage of 50 V. In this vicinity, there is good agreement between the calculated and experimental results. The noticeable discrepancies at low and high voltages can be explained by the fact that the only empirical parameter in the calculations was the electron momentum relaxation coefficient from the potential barrier in the boundary layer.

The boundary layer depth typical for electric propulsion plasma is approximately 1 micron. A cube with the same side length contains no more than a dozen electrons, making it impossible to solve the problem of electron behavior in this layer using continuum mechanics.

3.4. Discussion

The viscous transport of the azimuth projection of the electron momentum and the azimuth electron current in the radial direction into the cavity (represented by the radial-azimuth component of the

viscosity tensor $\pi_e^{(r\psi)}$) increases the skin depth compared to the classical theory, in which viscosity is not taken into account and the current is caused only by scattering in the volume.

Expressions (30) and (31) demonstrate a negative feedback loop between $\pi_e^{(r\psi)}$ on the one hand and $\partial/\partial r(V_{ea}/r)$ (the difference between the electron rotation and that of a solid) and $eB_a/m_e - V_{ea}/r$ (the locking of electron motion across magnetic lines) on the other hand. That is, in the limiting case of viscosity, the locking effect disappears ($eB_a/m_e - V_{ea}/r \rightarrow 0$) and the decrease in electron current as it moves deeper into the channel becomes smoother ($V_{e\psi} \sim r$) than in classical skin layer theory.

In the absence of conditions of occurrence of Trivelpiece-Gould waves, and also ICR and ECR, the expression (31) demonstrates an opportunity of occurrence of rotation-cyclotron resonance at equality of amplitudes of electrons angular velocity and cyclotron frequency from a variable component of a magnetic field.

The originality of the model presented in this paper lies in its being an integral part of the only currently available comprehensive plasma dynamic model of processes in a high-frequency hollow cathode. The calculation results presented here demonstrate qualitative agreement with measurements and can be used to predict operating parameters and narrow the range of parameters variations when developing laboratory models.

The limits and conditions of applicability of the model are determined by the specifics of the processes in electric propulsion devices, characterized by:

- the small size of the device compared to the mean free paths relative to all collision processes and the cyclotron radii of ions;
- the smallness of the cyclotron radii of electrons compared to the size of the device.

Thus, there are limitations in the application of the model to high-frequency ion-plasma technological devices; in some of them, the above conditions are not realized.

In future developments of high-frequency hollow cathodes, the values of this coefficient may be refined based on measurements in various operating modes.

4. Conclusions

1. The azimuth projection of the electron motion equation, taking into account the influence of a magnetic field on viscous momentum transport and viscous components of the electrons momentum flux density have been written, which permitted to analyze the viscous electrons momentum transport deeper into cathode cavity.

2. The equation of radial-azimuth component of electrons viscosity tensor has been written, which demonstrate the increase of skin layer depth comparatively with classic theory.

3. The expressions for electrons energy equation compounds, which represent the input of viscosity into process of electrons thermalization have been written, which allowed to close the mathematical model equations set. In the discharge current saturation region, in the anode circuit voltage range of 50–80 V, the difference between the calculated and measured current values does not exceed 3.5%. The noticeable difference in the low-voltage region is due to the transition process from the neutral to ionized states. In the high-voltage region, the superiority of the calculated current over the anode circuit current can be explained by its partial short-circuiting through the "vacuum chamber wall – voltage source" circuit. This drawback can be eliminated by increasing the size of the computational domain during simulation.

Conflict of interest

The author declares that he has no conflict of interest in relation to this research, whether financial, personal, author ship or otherwise, that could affect the research and its results presented in this paper.

Financing

This research was conducted without financial support.

Data availability

The manuscript has no associated data.

Use of artificial intelligence

The author confirms that he did not use artificial intelligence technologies when creating the current work.

Authors' contributions

Shahram Roshanpour: Methodology, Investigation, Formal analysis, Writing – original draft, Writing – review and editing.

References

1. Myers, R. M., Oleson, S. R., McGuire, M., Meckel, N. J., Cassady, R. J. (1995). Pulsed Plasma Thruster Technology for Small Satellite Missions. *The 9th AIAA, Utah State University Conference on Small Satellites*, 14. Available at: <https://ntrs.nasa.gov/api/citations/19960011377/downloads/19960011377.pdf>
2. Aoyagi, J., Hatakeyama, T., Irie, M., Okutsu, A., Takegahara, H., Watanabe, H. (2007). Preliminary Study on Radio Frequency Neutralizer for Ion Engine. *The 30th International Electric Propulsion Conf.*, 5. Available at: <https://electricrocket.org/IEPC/IEPC-2007-226.pdf>
3. Squire, J. P., Chang-Diaz, F. R., Jacobson, V. T., Glover, T. W., Baity, F. W., Carter, M. D. et al. (2003). Investigation of a Light Gas Helicon Plasma Source for the VASIMR Space Propulsion System. *AIP Conference Proceedings*, 694, 423–426. <https://doi.org/10.1063/1.1638071>
4. Zhu, Q., Su, Y. (2024). A Non-inductive Coil Design Used to Provide High-Frequency and Large Currents. *Sensors*, 24 (7), 2027. <https://doi.org/10.3390/s24072027>
5. Akhiezer, A. I., Akhiezer, I. A., Polovin, R. V., Sitenko, A. G., Stepanov, K. N. (2011). *Plasma Electrodynamics. Vol. 1. Linear Theory*. Pergamon press, 422. Available at: https://api.pageplace.de/preview/DT0400.9781483152158_A23873861/preview-9781483152158_A23873861.pdf
6. Shinohara, S. (2018). Helicon high-density plasma sources: physics and applications. *Advances in Physics: X*, 3 (1), 1420424. <https://doi.org/10.1080/23746149.2017.1420424>
7. Chen, F. F. (2001). Collisional, magnetic, and nonlinear skin effect in radio-frequency plasmas. *Physics of Plasmas*, 8 (6), 3008–3017. <https://doi.org/10.1063/1.1367322>
8. Korzec, D., Schott, M., Engemann, J. (1995). Radio frequency hollow cathode discharge for large-area double-sided foil processing. *Journal of Vacuum Science & Technology A: Vacuum, Surfaces, and Films*, 13 (3), 843–848. <https://doi.org/10.1116/1.579839>
9. Touš, J., Šícha, M., Hubička, Z., Soukup, L., Jastrabík, L., Čada, M., Tichý, M. (2002). The Radio Frequency Hollow Cathode Discharge Induced by the RF Discharge in the Plasma-Jet Chemical Reactor. *Contributions to Plasma Physics*, 42 (1), 119–131. [https://doi.org/10.1002/1521-3986\(200201\)42:1<119::aid-ctpp119>3.0.co;2-7](https://doi.org/10.1002/1521-3986(200201)42:1<119::aid-ctpp119>3.0.co;2-7)
10. Smirnov, P., Smirnova, M., Schein, J., Khartov, S. (2019). Research and development of radio-frequency cathode-neutralizer. *The 36th International Electric Propulsion Conference*, 7. Available at: <https://electricrocket.org/2019/840.pdf>
11. Roshanpur, S. (2013). Electron gas parameters change inside langmuir layer in electric propulsion devices. *Eastern-European Journal of Enterprise Technologies*, 4 (5 (64)), 36–39. <https://doi.org/10.15587/1729-4061.2013.16675>
12. Nesterenko, S., Zhihao, H., Roshanpour, S. (2025). Compromise kinetic-fluid model of electrons dynamics in electric propulsion devices with closed electrons drift as an alternative to the hybrid PIC-Fluid method. *Aerospace Technic and Technology*, 1, 28–37. <https://doi.org/10.32620/akt.2025.1.03>
13. Nesterenko, S. Yu., Roshanpour, Sh. (2013). Particles velocity distribution function moments equations set in rarified medium of inductive sources of plasma, electrons and ions. *Aviation and space engineering and technology*, 7 (104), 117–120. Available at: http://nbuv.gov.ua/UJRN/aktit_2013_7_23
14. Roshanpour, S. (2025). Viscous Absorption of Electromagnetic Capacity in Radio Frequency Low Current Hollow Cathode. *XIV Naukova konferentsiia "Naukovi Pidsumky 2025 Roku"*, 73. Available at: <https://entc.com.ua/download/HAYKOB1%20IIACYMKII%202025.pdf>
15. Roshanpour, S. (2025). Computer modeling of non-emission electron source with high-frequency ionization. *ScienceRise*, 2, 79–91. <https://doi.org/10.21303/2313-8416.2025.003885>

Shahram Roshanpour, Engineer/Researcher, IL SENTIERO INTERNATIONAL CAMPUS, Schio VI, Italy, e-mail: space.science@protonmail.com, ORCID: <https://orcid.org/0000-0002-4272-9217>